DOI: 10.1002/asia.200600107

VIP

Ultrafast Electron Diffraction: Structural Dynamics of Molecular Rearrangement in the NO Release from Nitrobenzene

Yonggang He, Andreas Gahlmann, Jonathan S. Feenstra, Sang Tae Park, and Ahmed H. Zewail*[a]

Abstract: Nitro compounds release NO, NO_2, and other species, but neither the structures during the reactions nor the time scales are known. Ultrafast electron diffraction (UED) allowed the study of the NO release from nitrobenzene, and the molecular pathways and the structures of the transient species were identified. It was observed, in contrast to previous inferences, that nitric oxide and phenoxyl radicals are formed dominantly and that the time scale of formation is 8.8 ± 2.2 ps. The structure of the phenoxyl radical was determined for the first time, and found to be quinoid-like. The mechanism proposed involves a repulsive triplet state, following intramolecular rearrangement. This efficient generation of NO may have important implications for the control of by-products in drug delivery and other applications.

Keywords: electron diffraction · elimination · femtochemistry · nitro compounds · structural dynamics

Introduction

Nitrobenzene, the prototypical member of a family of nitro compounds, is a common environmental pollutant[1–4] and a frequent ingredient in energetic explosives.[5] Elimination reaction pathways from nitrobenzene are known to produce NO_2, NO, and O radicals. The fragment nitric oxide (NO) is unique in that its mechanism of release may be relevant to the development of nitroaromatic NO donor drugs,[6,7] which are important in the regulation and maintenance of physiologically vital functions.[8–11] Even in the apparently simple reaction of NO loss from nitrobenzene, ambiguities continue to exist regarding the competition among reaction pathways, the various product yields, and the transient structures involved. Furthermore, an intramolecular rearrangement may occur in the release of NO and only with complete structural determination can we directly establish the pathways involved.

The phenoxyl radical, a resulting fragment of NO elimination from nitrobenzene, has been recognized as important in biological processes and combustion chemistry,[12,13] but its structure has not been determined. It has been the subject of both experimental and theoretical investigations, since it was observed as a reaction product in the vapor phase,[14] in solution,[15] and in a matrix.[16] The experimental information on phenoxyl has been provided by resonance Raman spectroscopy,[17–19] IR spectroscopy,[20,21] and ESR hyperfine couplings,[22–24] which led to the elucidation that C–O has double-bond character. Combined with the finding of a radical electron in the π ring system[23] and the known chemical reactivity of the phenoxyl radical, it was suggested that the ring of the phenoxyl radical is quinoid-like. Theoretical studies largely agree.[25,26]

Herein we report our first study of the structural dynamics of the elimination reaction of nitrobenzene by using ultrafast electron diffraction (UED) to determine transient structures directly. It is shown that the dominant pathway upon excitation is not that involving a single-bond rupture to produce NO_2 and a phenyl radical, but instead is a pathway of intramolecular rearrangement involving bond breaking and bond forming to yield NO and the phenoxyl radical (Scheme 1). This UED study sheds new light on the significant and long-debated problem regarding the reactions of nitroaromatic compounds by providing evidence of a dominant pathway, contrary to spectroscopic observations.

[a] Y. He, A. Gahlmann, J. S. Feenstra, S. T. Park, A. H. Zewail
Laboratory for Molecular Science and
Physical Biology Center for Ultrafast Science and Technology
California Institute of Technology
Pasadena, CA 91125 (USA)
Fax: (+1) 626-796-8315
E-mail: zewail@caltech.edu

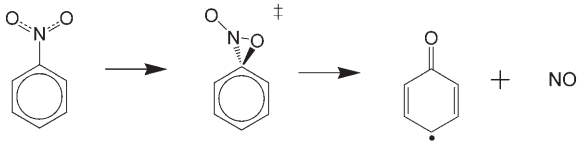

Scheme 1. Elimination reaction of nitrobenzene. The dominant pathway involves intramolecular rearrangement with bond breaking and bond forming to yield NO and the phenoxyl radical.

Results

The diffraction pattern of nitrobenzene in the ground state was directly recorded in two dimensions. This pattern was radial-averaged to give the one-dimensional curve, of which the sinusoidal oscillations contain all contributions from each internuclear distance. Refined structures were obtained by following our previously outlined methodology.[27,28] The experimental and the refined theoretical modified radial distribution, $f(r)$, and the molecular scattering function, $sM(s)$, are shown in Figure 1. The refined structural parameters, including the rotational barrier height, are compared to those from previous experiments as well as density functional theory (DFT) values (Table 1). They are in satisfactory agreement, with discrepancies within 0.02 Å and 1.5° for distances and angles, respectively. The exception lies with the nitro torsional angle values (ϕ) reported by Domenicano et al.[29] and by Shishkov et al.[30] These are $13.3 \pm 1.4°$ and 22.7°, respectively, and are strongly dependent on temperature. In these studies only a single torsional angle was employed for the internal rotation of the nitro group. When we use this approach, our data gives a value of 19.4°. This value represents $\langle|\phi|\rangle$, as positive and negative torsional angles are equivalent owing to the symmetry of the molecule. On the basis of the relation between this mean deviation and the potential $V_2 = RT/\pi\langle\phi\rangle^2$, Domenicano et al. estimated the rotational barrier to be around 4 ± 1 kcal mol^{-1}.[29]

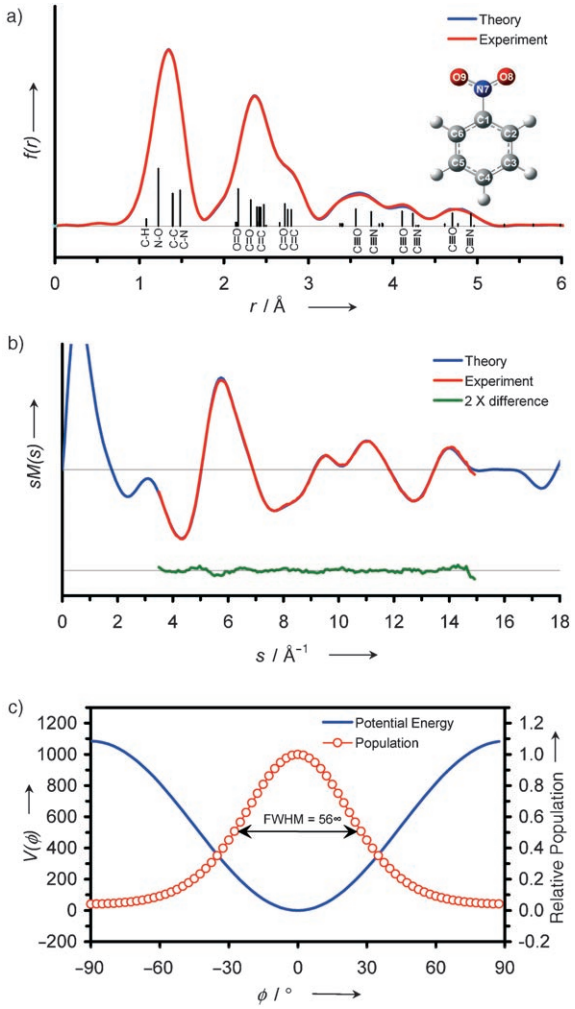

Figure 1. a) Radial distribution curve $f(r)$ (versus internuclear distance r), b) molecular scattering $sM(s)$ (as a function of momentum transfer s), and c) the rotation population and the potential energy (V) curve along the torsion angle (ϕ), for ground-state nitrobenzene. Theoretical (blue) and experimental (red) curves match with $R = 0.023$.

Owing to the low rotational barrier, the torsion of the nitro group was treated with explicit consideration of the large amplitude motion.[31] Thermal populations of internal rotational modes (with an angle binning of 2.5°) were evaluated with the potential function, $V = \frac{1}{2}V_0[1 - \cos(2\phi)]$, with the contribution of each angle being population-averaged. The shrinkage effect[32] and stretching anharmonicity were also incorporated. This dynamic model fixes the torsional angle at 0° with the standard deviation of the distribution (σ) defining the range of angles. From our data we obtain $\sigma = 28.7°$. Our structural refinement based on the dynamic model puts the rotational barrier at 3.1 ± 0.4 kcal mol^{-1}, in agreement with the values of 2.9 ± 0.2 kcal mol^{-1} and 3.3 kcal mol^{-1} obtained from microwave[33] and Raman spectroscopy[34] studies, respectively.

Table 1. The refined structure of ground-state nitrobenzene.

Parameters	Refined value[a]	Domenicano *et al*[b]	Shishkov *et al*[c]	Theoretical[d]
C1–C2, C6–C1	1.409 ± 0.009	1.3986	1.391	1.391
C2–C3, C5–C6	1.388 ± *0.024*[e]	1.3991		1.391
C3–C4, C4–C5	1.390 ± 0.009	1.3991		1.395
C–H	1.083	1.093	1.114	1.083
C1–N7	1.492 ± 0.001	1.486	1.478	1.481
N7–O8, N7–O9	1.219 ± 0.006	1.2234	1.218	1.223
C6–C1–C2	123.4 ± 0.8	123.4	125.1	122.3
C1–C2–C3, C5–C6–C1	117.3 ± *0.7*[e]	117.6	115.7	118.5
C2–C3–C4, C4–C5–C6	120.9 ± *0.7*[e]	120.6	122.5	120.2
C3–C4–C5	119.8 ± 0.6	120.18	118.3	120.3
C1–N7–O8, C1–N7–O9	116.4 ± 0.2	117.34	118.3	117.6
C2–C1–N7–O8	⟨0⟩ (28.7)[f]	⟨13.2⟩ (0)[f]	⟨22.7⟩ (0)[f]	0
V_2 [kcal mol^{-1}][g]	3.1 ± 0.4	4	1.3	6.5

[a] C_{2v} symmetry was used during the structural refinement. The error bars reported are 3σ. [b] Taken from reference [29]. [c] Taken from reference [30]. [d] Theoretical structures were obtained by using DFT calculations at the B3LYP/6-311G(d, p) level of theory. [e] Dependent variables and propagated errors. [f] Angle brackets denote the center values, parenthesis indicate the population-weighted standard deviation (see text for details). [g] V_2 denotes rotational barrier along the torsional motion of the nitro group.

To study structural dynamics during the course of the reaction, we recorded time-resolved diffraction patterns at different times, from −100 ps to +100 ps in one set of experiments, and from −100 ps to +1 ns in other sets of experiments. To identify the reaction channel(s) upon excitation at 266.7 nm, the experimental and theoretical $\Delta sM(s)$ and $\Delta f(r)$ curves for energetically allowed channels (Figure 2), as well as their multiple combinations, were compared. Vibrational temperatures of each of the products were estimated by using calculated vibrational frequencies and available energies. Mean translational energy release and rotational energy partitioning were also taken into account.[35]

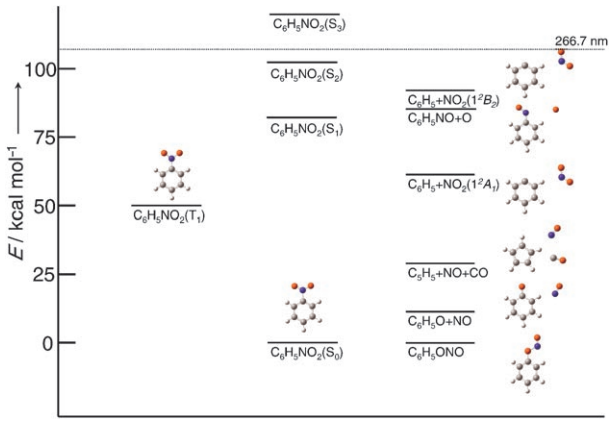

Figure 2. Energy diagram of excited states and chemical channels of nitrobenzene.

Figure 3 displays the comparison of the experimental $\Delta f(r)$ curves with theory at the +1-ns time delay (reference at −100 ps). Theoretical structures that matched the data poorly were excluded. The experimental $\Delta sM(s)$ and $\Delta f(r)$

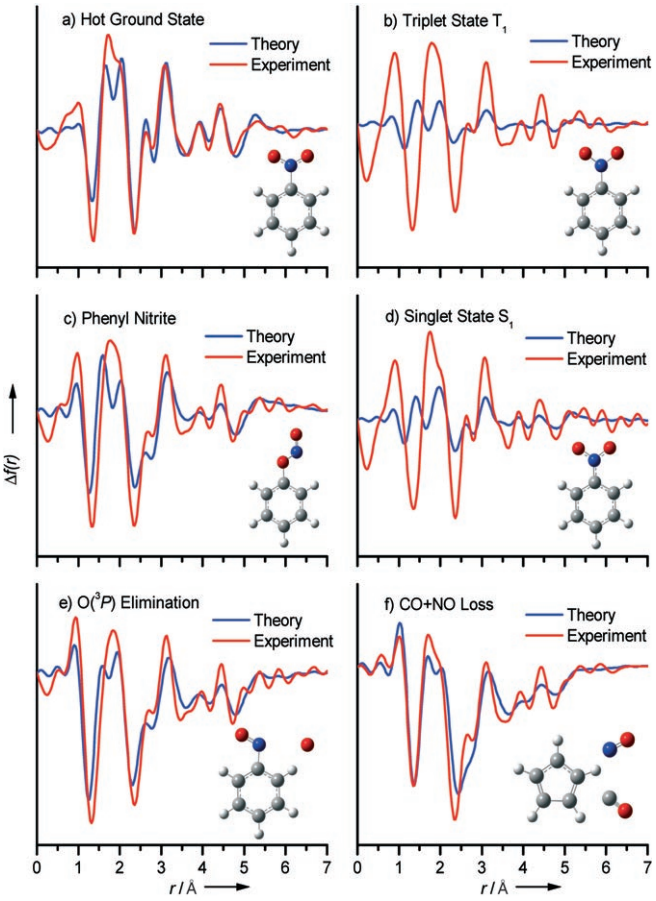

Figure 3. Radial distribution curves $\Delta f(r; t = +1\ \text{ns}, t_{\text{ref}} = -100\ \text{ps})$ for trial fits of different reaction pathways. The product channels are: a) "hot" ground state $C_6H_5NO_2$; b) triplet (T_1, $^3\pi$–π^*) $C_6H_5NO_2$; c) phenyl nitrite (C_6H_5ONO); d) S_1 (^{1}n–π^*) $C_6H_5NO_2$; e) $C_6H_5NO + O$ (^3P); and f) $C_5H_5 + CO + NO$.

curves for NO_2 eliminations (with the ground and the excited states of the NO_2 fragment) and NO elimination are highlighted in Figure 4. Structural refinement attempted for these NO_2 channels resulted in unphysical structures. The best fit was obtained when using $C_6H_5NO_2 \rightarrow C_6H_5O + NO$ as the dominant reaction. Multicomponent fits (not shown) performed by floating the fraction of several channels also favored an exclusive NO-elimination reaction. Similar results were also found at both +50-ps and +100-ps time delays. These results establish that the dominant reaction channel of nitrobenzene upon excitation at 266.7 nm is NO elimination. With the reaction channel identified, the structure of its corresponding product, the phenoxyl radical, was then refined. Figure 5 shows the experimental and the refined theoretical molecular scattering and radial distribution curves for the NO-elimination reaction channel. The refined

CHEMISTRY
AN ASIAN JOURNAL

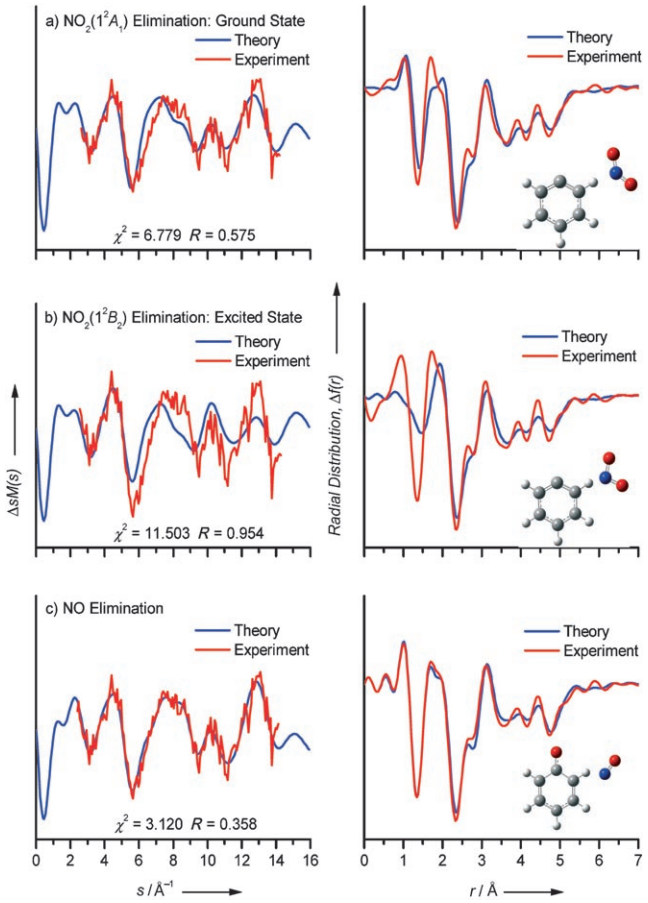

Figure 4. Molecular scattering curves, $\Delta sM(s;t=+1\text{ ns}, t_{ref}=-100\text{ ps})$, and radial distribution curves, $\Delta f(r;t=+1\text{ ns}, t_{ref}=-100\text{ ps})$, for trial fits of NO_2- and NO-elimination reactions: a) $C_6H_5+NO_2$ (1^2A_1); b) $C_6H_5+NO_2$ (1^2B_2); and c) C_6H_5O + NO.

structural parameters are listed in Table 2 together with DFT values. The C–O bond length was found to be 1.232 Å. Aryl C–C bonds are 1.465 Å, 1.382 Å, and 1.420 Å at their primary, secondary, and tertiary positions (with respect to the O atom), giving the average value of 1.423 Å.

Table 2. The refined structures of intermediates.

Species	Parameters	Refined value[a]	Theoretical[b]
nitric oxide	N–O	1.148	1.148
phenoxyl	C1–C2, C6–C1	1.465 ± 0.018[c]	1.452
	C2–C3, C5–C6	1.382 ± 0.018[c]	1.375
	C3–C4, C4–C5	1.420 ± 0.018[c]	1.408
	C–H	1.084	1.084
	C1–O7	1.232 ± 0.064	1.251
	C6–C1–C2	116.9	116.9
	C1–C2–C3, C5–C6–C1	121.0	121.0
	C2–C3–C4, C4–C5–C6	120.2	120.2
	C3–C4–C5	120.7	120.7

[a] C_{2v} symmetry was used for the phenoxyl radical. The N–O bond length of nitric oxide and all structural parameters involving hydrogen atoms were fixed at DFT-calculated values. Only two structural parameters, the C–O bond length and the mean ring C–C bond length, were refined owing to correlation difficulties; the individual ring C–C lengths were defined from the mean refined value. The error bars reported are 3σ. [b] Theoretical structures were obtained by DFT calculations at the B3LYP/6-311G(d, p) level of theory. [c] Dependent variables and propagated errors.

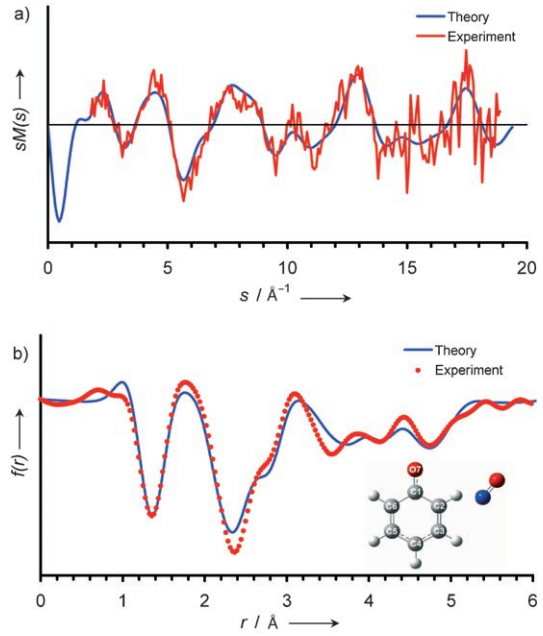

Figure 5. a) Frame-referenced modified molecular scattering curves, $\Delta sM(s;t)$, and b) frame-referenced radial distributions, $\Delta f(r;t)$ for nitrobenzene (266.7 nm excitation) at $t=+1$ ns ($t_{ref}=-100$ ps) along with the refined theoretical curves corresponding to the reaction products phenoxyl and NO radicals. The experimental data points are shown as a red line and the refined theory is a blue line ($R=0.375$).

From the temporal frame-referenced diffraction data, the population of the product structures as a function of time was determined. Figure 6 displays the 1D frame-referenced radial distribution curves from −100 to +100 ps. The curves clearly map out the reaction showing both negative peaks (blue regions), which correspond to the loss of old bonds, and positive peaks (red regions) corresponding to the formation of new bonds. The curves retain the same features over time, but simply increase in amplitude, indicating the growth in population of a common product structure. Figure 7 shows the growth of the product fraction with time. Nonlinear fitting, for a single-step reaction, gives a rise time of 8.8 ± 2.2 ps.

Discussion

Previous Spectroscopic Studies

Spectroscopic characterization of nitrobenzene has been the subject of study for decades. The gas-phase UV absorption spectrum of nitrobenzene consists of three broad and structureless bands, centered at 280 nm, 240 nm, and 195 nm.[36–39] A much weaker absorption band at ≈350 nm was also observed.[40] Excitation to these states results in no observable fluorescence or phosphorescence. An early gas-phase study assigned the 240-nm band to be a charge-transfer state from the phenyl ring to the NO_2 moiety.[36] A similar conclusion

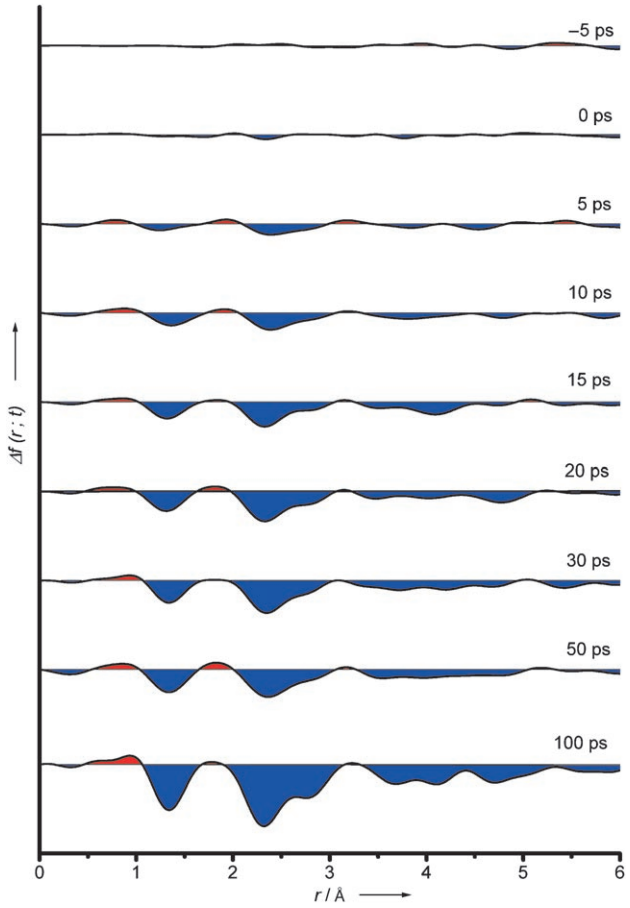

Figure 6. The experimental $\Delta f(r;t)$ with the time steps indicated. Negative peaks (blue regions) correspond to the loss of old bonds; positive peaks (red regions) correspond to the formation of new bonds.

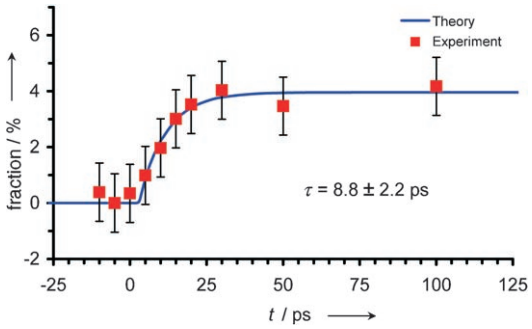

Figure 7. The temporal dependence of the product fraction in the reaction $C_6H_5NO_2 \rightarrow C_6H_5O + NO$. Nonlinear fitting of a single-step reaction yields a time constant of 8.8 ± 2.2 ps.

was also made by other experimental and theoretical investigations.[41,42] However, polarization spectroscopy indicates that the 240-nm band is characterized by a transition dipole moment that is mostly perpendicular to the molecular figure axis, whereas that of the 280-nm band was inferred to be parallel, providing contrary evidence to some previous spectroscopic and theoretical assignments.[38,39] The energy of the lowest triplet state in solution was deduced to be 58 kcal mol^{-1}.[43] The photophysical dynamics of nitrobenzene is fairly limited. The lifetime of the triplet upon excitation at $\approx$366 nm in liquids was deduced to be $\approx$1 ns from the measurement of intersystem crossing (ISC) yield by using photosensitization.[44] The lifetime of the lowest excited singlet state (S_1) was found to be 6 ps and that of presumably the lowest triplet state (T_1) to be 400–900 ps depending on the solvent, with an ISC yield of 0.8.[45–47]

The rich photochemistry of nitrobenzene has been reported in the vapor,[37,48–56] in solutions,[57] and in matrices.[13,20,21] Early discharge-lamp studies detected NO_2 and C_6H_5NO as photodissociation products,[48,49] suggesting two reaction processes: $C_6H_5NO_2 \rightarrow C_6H_5 + NO_2$ and $C_6H_5NO_2 \rightarrow C_6H_5NO + O$. Flash photolysis has also led to C_5H_5 as a product.[50] A number of mass spectrometry studies on the photodissociation of nitrobenzene by using nanosecond laser pulses at various wavelengths revealed the coexistence of multiple dissociation channels, including those yielding NO_2, O, and NO.[37,52,54–56] Pyrolysis by pulsed IR laser heating showed C_6H_5–NO_2 bond breaking to be the primary reaction channel.[51] Another pyrolysis study by using a single-pulse shock tube method identified the formation of phenoxyl radical as a minor channel.[53]

In spite of these extensive photodissociation studies, the lack of ionization cross-section data has hindered the quantitative analysis of the branching ratio among the reaction channels. On the basis of ion signal-intensity data, NO elimination had been considered a relatively minor reaction.[37,54,55] Assuming that both NO_2 and NO are produced in the ground state, Galloway et al. estimated the branching ratio between NO_2 and NO elimination to range from 1.3 to 5.9 for excitation wavelengths between 280 and 222 nm, by using ion signal intensities detected and the single photon ionization cross-sections from ground states.[37] Because NO_2 may form in the excited state,[37,48] the authors[37] noted that the branching ratio should be viewed as an upper limit; excited NO_2 supposedly has a higher ionization efficiency.

Structural Dynamics from UED

The structural dynamics reported herein obtained by using UED indicate the dominance of the NO-elimination channel at 266.7 nm. Our result would be consistent with the spectroscopic analysis only if NO_2 is generated in the excited state. However, its yield relative to NO must be very low; the apparent enhanced detection is due to the presumed higher cross-section for ionization from excited NO_2 and the ratio of yield to NO becomes less than 1. Also consistent with our findings are the results of infrared studies of photoexcited nitrobenzene in an Ar matrix,[21] which report the exclusive observation of a weakly bound $C_6H_5O\cdots NO$ complex, whereas those corresponding to O and NO_2 eliminations were not found. The refined structure of the phenoxyl radical with strong C–O double-bond character (1.232 ± 0.064 Å) is in agreement with the values obtained

from DFT (1.253–1.270 Å),[26,58–60] as well as CASSCF/6-311G(2*d*,*p*) (1.228 Å) calculations.[25,26] The refined C–C bond lengths of the phenyl ring, in general, agree with previous high-level calculations: the C1–C2 (1.465 Å) and C2–C3 (1.382 Å) bond lengths are close in value to typical C–C single and double bonds, respectively, while the C3–C4 bond length (1.420 Å) shows partial double-bond character, quinoid-like, resulting from the conjugation effect of the radical center.

The rise time for the formation of the phenoxyl and NO radicals from UED is 8.8 ps. At our wavelength, the molecule is excited to a high-energy state (see previous subsection) which, as is known from photophysical studies, does not fluoresce. Relative yields and product-energy partitioning, measured between 320 and 240 nm, show no abrupt change over the range,[35,37] and, therefore, it is reasonable to deduce that excitation to states higher than S_1 results in an efficient internal conversion (IC), as we reported elsewhere for related systems.[28,61] Moreover, vapor-phase nitroaromatic compounds in S_1 (>300 nm) undergo highly efficient ISC.[62] In the liquid phase, the ISC yield of nitrobenzene has been determined to be greater than 0.80, and the lifetime of the S_1 state to be 6 ps at 320 nm.[45,63] This ultrafast ISC can be rationalized by the proximity effect[64] and efficient one-center overlap between S_1 (n–π*) and T_1 (π–π*).[65] Accordingly, the rise time of 8.8 ps covers both the rates of ISC and the triplet-state reaction yielding NO and phenoxyl radicals (Figure 8). The barrier to NO release

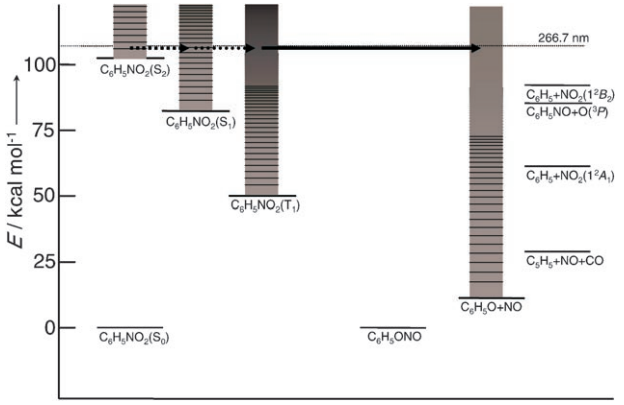

Figure 8. Possible photophysical and photochemical pathways of nitrobenzene upon excitation at 266.7 nm.

from T_1 was calculated (see below), from which the statistical time constant for the formation of products was determined to be ≈1 ns. However, the reaction time becomes ≈1 ps when considering a directed motion involving only "local" modes.

To examine the nature of potential surfaces and reaction rates, we performed DFT calculations of the likely nuclear motions for the rearrangement–elimination process on both T_1 and S_0 (Figure 9);[66] The S_0 surface has been invoked to describe pyrolysis reactions,[51,53,67–69] but the results do not agree with the photochemical behavior of nitrobenzene.[35,67]

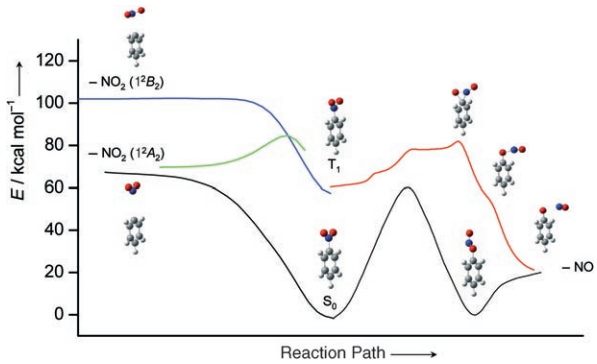

Figure 9. Theoretical calculations of the S_0 and T_1 surfaces for NO and NO_2 eliminations (see text).

For comparison, the $C_6H_5+NO_2$ pathway is also presented in Figure 9. The T_1 state is mainly of $^3\pi$–π^* character localized on the nitro group. Thus, direct C–N bond scission adiabatically correlates with an excited NO_2 (1^2B_2) and a ground-state phenyl radical. This is affirmed by our calculation, which predicts that no direct pathway leading to phenyl radical + NO_2 (1^2A_1) exists on the T_1 surface. Furthermore, NO_2 (1^2B_2) elimination involves the surmounting of a high barrier (≈45 kcal mol^{-1}). These findings are consistent with the negligible contribution of the NO_2-elimination channel in our data, and also with the high yield of NO_2 ion signal reported previously by Galloway et al.[37,48] The loose character of the C–N cleavage transition state explains the small relative translational energy partitioning into the fragments and the yield increase with photon energy.[37] The production of excited NO_2 has been seen in the photodissociation of nitromethane at 193 nm.[70,71]

In contrast to the dissociation producing NO_2 (1^2B_2), NO elimination on T_1 involves a lower-energy barrier (≈25 kcal mol^{-1}) and a large exothermic energy change owing to the stability of the phenoxyl radical. This relatively low barrier explains its dominance over the other channels. Since phenyl nitrite, the NO elimination intermediate structure on S_0, is not stable on the T_1 surface, the exit channel from the TS is direct and efficiently results in phenoxyl and NO radicals. The exit channel barrier is rather high (2.64 eV), consistent with the product energy partitioning reported from multiphoton ionization (MPI) and laser-induced fluorescence (LIF) studies[35,68,72] of the NO product (translational energy = 1.1, 0.86, and 0.56 eV at 226, 240, and 280 nm excitation, respectively, and rotational energy = 0.32 and 0.20 eV at 226 and 280 nm excitation, respectively).[35] In an orbital valence-bond description, the $^3\pi$–π^* excitation generates an unpaired electron on each oxygen atom. Rotation of the nitro moiety then results in favorable overlap of the nonbonding orbital of the O atom (in the plane of NO_2) with the adjacent π orbital of the aromatic ring and forms the pseudo-three-membered ring. The R–N–O bonds with weakened π bonding ($^3\pi$–π^*) are severed as the new C–O bond is formed.

Conclusions

Structural dynamics obtained directly with UED reveal that NO release in 8.8 ps involves intramolecular rearrangement and is the dominant elimination reaction pathway. The structure of the transient phenoxyl radical was determined, and, with the aid of theory, the reaction pathway was suggested to involve the lowest triplet potential-energy surface. A quantitative determination of the time-dependent populations of individual product species was obtained by resolving their transient structures. This advantage, absent in previous spectroscopic studies, dispels the uncertainty regarding the reaction mechanism. In contrast to pyrolysis in the ground state, which leads to various by-products, the dominance of NO release on the triplet surface may be utilized in designing effective NO-delivering drugs with minimized side reactions (NO_2 release, for example). It may also assist in studies of atmospheric nitroaromatic compounds.[72]

Experimental Section

A detailed description of the UED III apparatus and data analysis has been given in previous publications.[27,28] Briefly, ultrashort laser pulses of 120 fs at 800 nm were frequency-tripled. The resulting UV light (450 μJ/pulse) was split into two beam paths. The pump beam ($\approx$93% of the total energy, time delayed by using a translation stage) was focused to a size of $\approx$400 μm in diameter and directed into the scattering chamber to initiate the reaction. The weaker beam ($\approx$7% of the total energy) was attenuated, focused, and directed onto a back-illuminated silver-coated cathode to yield ultrashort electron pulses through the photoelectric effect. The electron pulses were accelerated at 30 keV ($\lambda_{\text{de Broglie}}$ = 0.067 Å) to form a beam with a size at fwhm (full width at half maximum) of $\approx$370 μm and were then directed through the molecular beam. Zero-of-time was established by maximizing the lensing effect[73,74] with 1,3-butadiene.

For the present study, two separate experiments were performed: A full series of time-resolved diffraction patterns were obtained to determine the reaction dynamics (3.1×10^4 electrons/pulse, 5 ps pulse width). Another series of patterns was also taken with more electrons per pulse and fewer time points (data collected at four time points) to determine the structure of the transient species (8.8×10^4 electrons/pulse, 11 ps pulse width). The temperature was increased progressively from the sample reservoir through the manifold to the needle tip, from 433 K to 493 K, in order to avoid condensation. The sample vapor enters the chamber through a 180-μm aperture by effusive expansion to form a molecular beam with an estimated fwhm of $\approx$325 μm at the interaction region. Nitrobenzene (>99%) was purchased from Aldrich and used without further purification.

For the study of transient structures, diffraction patterns were recorded at different time delays between initiating laser pulse and electron pulse. Temporal frame-referenced data were then generated by subtracting the reference diffraction pattern recorded before time-zero (t_{ref} = −100 ps) from patterns obtained at all other time delays.

The starting geometries for structural analysis were obtained by quantum chemical calculations using DFT at the B3LYP/6-311G(d,p) level (Gaussian 98 suite).[75] Structural analysis was conducted on home-built software using previously described methodology.[28]

Acknowledgements

We thank the National Science Foundation and the Air Force Office of Scientific Research for providing support for this work.

[1] W. M. Schackelford, D. M. Cline, L. Faas, G. Kurth, *Anal. Chim. Acta* **1983**, *146*, 15.
[2] H. F. Mark, D. F. Othmer, C. G. Overberger, G. T. Seaburg, *Kirk-Othmer Encyclopedia of Chemical Technology, 4th ed.*, Wiley, New York, **1992**.
[3] K. Hayward, *Water* **1999**, *21*, 4.
[4] R. Atkinson, E. C. Tuazon, T. J. Wallington, S. M. Aschmann, J. Arey, A. M. Winer, J. N. Pitts, *Environ. Sci. Technol.* **1987**, *21*, 64.
[5] T. B. Brill, K. J. James, *Chem. Rev.* **1993**, *93*, 2667.
[6] K. Fukuhara, M. Kurihara, N. Miyata, *J. Am. Chem. Soc.* **2001**, *123*, 8662.
[7] T. Suzuki, O. Nagae, Y. Kato, H. Nakagawa, K. Fukuhara, N. Miyata, *J. Am. Chem. Soc.* **2005**, *127*, 11720.
[8] F. Murad, *Angew. Chem. Int. Ed.* **1999**, *38*, 1856; *Angew. Chem.* **1999**, *111*, 1976.
[9] R. F. Furchgott, *Angew. Chem. Int. Ed.* **1999**, *38*, 1870; *Angew. Chem.* **1999**, *111*, 1990.
[10] L. J. Ignarro, *Angew. Chem. Int. Ed.* **1999**, *38*, 1882; *Angew. Chem.* **1999**, *111*, 2002.
[11] P. G. Wang, M. Xian, X. Tang, X. Wu, Z. Wen, T. Cai, A. J. Janczuk, *Chem. Rev.* **2002**, *102*, 1091.
[12] K. Tonokura, T. Ogura, M. Koshi, *J. Phys. Chem. A* **2004**, *108*, 7801.
[13] J. Spanget-Larsen, M. Gil, A. Gorski, D. M. Blake, J. Waluk, J. G. Radziszewski, *J. Am. Chem. Soc.* **2001**, *123*, 11253.
[14] G. Porter, F. J. Wright, *Trans. Faraday Soc.* **1955**, *51*, 1469.
[15] E. J. Land, G. Porter, E. Strachan, *Trans. Faraday Soc.* **1961**, *57*, 1885.
[16] J. L. Roebber, *J. Chem. Phys.* **1962**, *37*, 1974.
[17] S. M. Beck, L. E. Brus, *J. Chem. Phys.* **1982**, *76*, 4700.
[18] G. N. R. Tripathi, R. H. Schuler, *J. Chem. Phys.* **1984**, *81*, 113.
[19] A. Mukherjee, M. L. McGlashen, T. G. Spiro, *J. Phys. Chem.* **1995**, *99*, 4912.
[20] J. G. Radziszewski, M. Gil, A. Gorski, J. Spanget-Larsen, J. Waluk, B. J. Mróz, *J. Chem. Phys.* **2001**, *115*, 9733.
[21] R. Yang, X. Jin, W. Wang, K. Fan, M. Zhou, *J. Phys. Chem. A* **2005**, *109*, 4261.
[22] W. T. Dixon, R. O. C. Norman, *J. Chem. Soc.* **1964**, 4857.
[23] T. J. Stone, W. A. Waters, *J. Chem. Soc.* **1964**, 213.
[24] W. T. Dixon, D. Murphy, *J. Chem. Soc. Faraday Trans. 2* **1976**, *72*, 1221.
[25] D. M. Chipman, R. Liu, X. Zhou, P. Pulay, *J. Chem. Phys.* **1994**, *100*, 5023.
[26] Y. Qin, R. A. Wheeler, *J. Chem. Phys.* **1995**, *102*, 1689.
[27] R. Srinivasan, V. A. Lobastov, C. Y. Ruan, A. H. Zewail, *Helv. Chim. Acta* **2003**, *86*, 1763.
[28] S. T. Park, J. S. Feenstra, A. H. Zewail, *J. Chem. Phys.* **2006**, *124*, 174707.
[29] A. Domenicano, G. Schultz, I. Hargittai, M. Colapietro, G. Portalone, P. George, C. W. Bock, *Struct. Chem.* **1990**, *1*, 107.
[30] I. F. Shishkov, N. I. Sadova, V. P. Novikov, L. V. Vilkov, *Zh. Strukt. Khim.* **1984**, *25*, 98.
[31] T. Tsuji, H. Takashima, H. Takeuchi, T. Egawa, S. Konaka, *J. Phys. Chem. A* **2001**, *105*, 9347.
[32] V. A. Sipachev, *THEOCHEM* **1985**, *121*, 143.
[33] J. H. Høg, Ph. D. thesis, University of Copenhagen, Copenhagen, Denmark, **1971**.
[34] L. A. Carreira, T. G. Towns, *J. Mol. Struct.* **1977**, *41*, 1.
[35] D. B. Galloway, T. Glenewinkel-Meyer, J. A. Bartz, L. G. Huey, F. F. Crim, *J. Chem. Phys.* **1994**, *100*, 1946.
[36] S. Nagakura, M. Kojima, Y. Maruyama, *J. Mol. Spectrosc.* **1964**, *13*, 174.
[37] D. B. Galloway, J. A. Bartz, L. G. Huey, F. F. Crim, *J. Chem. Phys.* **1993**, *98*, 2107.

[38] K. J. Castle, J. Abbott, X. Peng, W. Kong, *J. Chem. Phys.* **2000**, *113*, 1415.
[39] J. E. Abbott, X. Peng, W. Kong, *J. Chem. Phys.* **2002**, *117*, 8670.
[40] B. Vidal, J. N. Murrell, *Chem. Phys. Lett.* **1975**, *31*, 46.
[41] M. B. Robin, *Higher excited states of polyatomic molecules, Vol. 2*, Academic Press, New York, **1975**.
[42] O. Kröhl, K. Malsch, P. Swiderek, *Phys. Chem. Chem. Phys.* **2000**, *2*, 947.
[43] R. W. Yip, D. K. Sharma, R. Giasson, D. Gravel, *J. Phys. Chem.* **1984**, *88*, 5770.
[44] R. Hurley, A. C. Testa, *J. Am. Chem. Soc.* **1968**, *90*, 1949.
[45] M. Takezaki, N. Hirota, M. Terazima, *J. Phys. Chem. A* **1997**, *101*, 3443.
[46] M. Takezaki, N. Hirota, M. Terazima, H. Sato, T. Nakajima, S. Kato, *J. Phys. Chem. A* **1997**, *101*, 5190.
[47] M. Takezaki, N. Hirota, M. Terazima, *J. Chem. Phys.* **1998**, *108*, 4685.
[48] V. H. Schuler, A. Woeldike, *Phys. Z.* **1944**, *45*, 171.
[49] S. H. Hastings, F. A. Matsen, *J. Am. Chem. Soc.* **1948**, *70*, 3514.
[50] G. Porter, B. Ward, *Proc. R. Soc. London Ser. A* **1968**, *303*, 139.
[51] A. C. Gonzalez, C. W. Larson, D. F. McMillen, D. M. Golden, *J . Phys. Chem.* **1985**, *89*, 4809.
[52] E. C. Apel, N. S. Nogar, *Int. J. Mass Spectrom. Ion Processes* **1986**, *70*, 243.
[53] W. Tsang, D. Robaugh, W. G. Mallard, *J. Phys. Chem.* **1986**, *90*, 5968.
[54] A. Marshall, A. Clark, R. Jennings, K. W. D. Ledingham, J. Sander, R. P. Singhal, *Int. J. Mass Spectrom. Ion Processes* **1992**, *116*, 143.
[55] A. Marshall, A. Clark, R. Jennings, K. W. D. Ledingham, R. P. Singhal, *Int. J. Mass Spectrom. Ion Processes* **1992**, *112*, 273.
[56] C. Kosmidis, K. W. D. Ledingham, A. Clark, A. Marshall, R. Jennings, J. Sander, R. P. Singhal, *Int. J. Mass Spectrom. Ion Processes* **1994**, *135*, 229.
[57] X.-M. Zhu, S.-Q. Zhang, X. Zheng, D. L. Phillips, *J. Phys. Chem. A* **2005**, *109*, 3086.
[58] O. Nwobi, J. Higgins, X. Zhou, R. Liu, *Chem. Phys. Lett.* **1997**, *272*, 155.
[59] C. Adamo, R. Subra, A. Di Matteo, V. Barone, *J. Chem. Phys.* **1998**, *109*, 10244.
[60] R. Schnepf, A. Sokolowski, J. Müller, V. Bachler, K. Wieghardt, P. Hildebrandt, *J. Am. Chem. Soc.* **1998**, *120*, 2352.
[61] J. S. Feenstra, S. T. Park, A. H. Zewail, *J. Chem. Phys.* **2005**, *123*, 221104.
[62] M. Kasha, *Radiat. Res. Suppl.* **1960**, *2*, 243.
[63] M. Takezaki, N. Hirota, M. Terazima, *Prog. Nat. Sci.* **1996**, *6*, S453.
[64] E. C. Lim, *J. Phys. Chem.* **1986**, *90*, 6770.
[65] M. A. El-Sayed, *J. Chem. Phys.* **1963**, *38*, 2834.
[66] The zero-point energy is not incorporated in the calculation of potential-energy curves along the intrinsic reaction coordinate. For open-shell DFT calculations the errors may, in this case, result in underestimation of some product energies by $\approx 10\,\mathrm{kcal\,mol^{-1}}$ or less. The energy of T_1 in THF is $58\,\mathrm{kcal\,mol^{-1}}$.[43] The experimental changes in enthalpy at 0 K are 21 ± 1, 76 ± 2, and $103 \pm 2\,\mathrm{kcal\,mol^{-1}}$ for NO, NO_2 (1^2A_1), and NO_2 (1^2B_2) channels, respectively, which were evaluated from the enthalpies of formation at 298 K given by the National Institute of Standards and Technology (NIST) Standard Reference Database Number 69 and corrected to 0 K values by using DFT frequencies. The obtained DFT values are 55, 15, 66, and $93\,\mathrm{kcal\,mol^{-1}}$, respectively. T_1 values are 57 and $66\,\mathrm{kcal\,mol^{-1}}$ from CASSCF and MCQDPT, respectively, and 55 and $58\,\mathrm{kcal\,mol^{-1}}$ from references [42] and [46], respectively.
[67] T. Glenewinkel-Meyer, F. F. Crim, *THEOCHEM* **1995**, *337*, 209.
[68] Y.-M. Li, J.-L. Sun, H.-M. Yin, K.-L. Han, G.-Z. He, *J. Chem. Phys.* **2003**, *118*, 6244.
[69] S. Xu, M. C. Lin, *J. Phys. Chem. B* **2005**, *109*, 8367.
[70] L. J. Butler, D. Krajnovich, Y. T. Lee, G. Ondrey, R. Bersohn, *J. Chem. Phys.* **1983**, *79*, 1708.
[71] K. Q. Lao, E. Jensen, P. W. Kash, L. J. Butler, *J. Chem. Phys.* **1990**, *93*, 3958.
[72] N. Daugey, J. Shu, I. Bar, S. Rosenwaks, *Appl. Spectrosc.* **1999**, *53*, 57.
[73] M. Dantus, S. B. Kim, J. C. Williamson, A. H. Zewail, *J. Phys. Chem.* **1994**, *98*, 2782.
[74] J. C. Williamson, J. Cao, H. Ihee, H. Frey, A. H. Zewail, *Nature* **1997**, *386*, 159.
[75] Gaussian 98 (Revision A.9), M. J. Frisch, G. W. Trucks, H. B. Schlegel, G. E. Scuseria, M. A. Robb, J. R. Cheeseman, V. G. Zakzrewski, J. A. Montegomery, R. E. Stratmann, J. C. Burant, S. Dapprich, J. M. Milliam, A. D. Daniels, K. N. Kudin, B. Mennuci, C. Pomelli, C. Adamo, S. Clifford, J. Ochtersi, G. A. Patterson, P. Y. Ayala, Q. Cui, K. Morokuma, D. K. Malick, A. D. Rabuck, K. Raghavachari, J. B. Foresman, J. Cioslowski, J. V. Ortiz, B. B. Stefanov, G. Liu, A. Liashenko, P. Piskorz, I. Komaromi, R. Gomperts, R. L. Martin, D. J. Fox, T. Kieth, M. A. Al-Laham, C. Y. Peng, A. Nanayakkara, G. Gonzales, M. Challacombe, P. M. W. Gill, B. G. Johnson, W. C. Wong, M. W. Wong, J. L. Andres, M. Head-Gordon, E. S. Replogle, J. A. Pople, Gaussian Inc., Pittsburgh, PA, **1998**.

Received: March 24, 2006
Published online: July 3, 2006

